Aerosol and Air Quality Research, 18: 1631–1641, 2018

ISSN: 1680-8584 print / 2071-1409 online
doi: 10.4209/aaqr.2017.07.0248

Temporal Variation of Atmospheric Static Electric Field and Air Ions and their Relationships to Pollution in Shanghai

Yifan Wang[1], Yanyu Wang[1], Junyan Duan[1], Tiantao Cheng[1,2,3*], Hailin Zhu[1], Xin Xie[1], Yuehui Liu[1], Yan Ling[1], Xiang Li[1], Hongli Wang[2], Mei Li[3], Renjian Zhang[4]

[1] Shanghai Key Laboratory of Atmospheric Particle Pollution and Prevention (LAP[3]), Department of Environmental Science and Engineering, Institute of Atmospheric Sciences, Fudan University, Shanghai 200433, China
[2] State Environmental Protection Key Laboratory of Formation and Prevention of Urban Air Pollution Complex, Institute of Atmospheric Environment, Shanghai Academy of Environmental Sciences, Shanghai 200233, China
[3] Guangdong Engineering Research Center for Online Atmospheric Pollution Source Apportionment Mass Spectrometry System, Institute of Mass Spectrometer and Atmospheric Environment, Jinan University, Guangzhou 510632, China
[4] Key Laboratory of Region Climate-Environment Research for Temperate East Asia (CAS-TEA), Institute of Atmospheric Physics, Chinese Academy of Sciences, Beijing 100029, China

ABSTRACT

Atmospheric electric field (EF) and air ions were measured in Shanghai from December 2014 to December 2015 to examine the influence of particulate pollutants. Fair-weather EF exhibits a diurnal variation of multi-modal oscillations in spring, summer, and autumn. Linear correlation analyses show that the local meteorological conditions of relative humidity, temperature, pressure and wind affect atmospheric electric field, with wind direction exhibiting the highest correlation coefficient. Atmospheric EF is significantly higher in the west compared with that in the east, as the air mass from inland areas carries more polluted aerosols. Air ion concentrations are generally higher in the daytime than at night and correlate with meteorological factors. Atmospheric EF undergoes a substantial fluctuation in polluted periods, but remains flat under clean conditions. Overall, in areas with pollution, the atmospheric EF gradually increases with increased pollution or increased particle loading (e.g., $PM_{2.5}$), a useful indicator of air pollution.

The concentration of $PM_{2.5}$ is positively correlated with the atmospheric electric field under polluted conditions, because as the concentration of aerosol particles declines, the concentrations of small ions and the atmospheric conductivity decrease accordingly, thus causing an increase in the electric field. Overall, aerosol particles, air ions, and their interactions in the presence of various meteorological parameters can have local effects on the atmospheric electric field.

Keywords: Atmospheric electric field; Air ions; Urban pollution.

INTRODUCTION

An electric potential difference of about 250 kV between the ground and the ionosphere produces a vertical downward atmospheric electric field (EF) at the surface of the earth. The ground-level vertical component of the EF may be divided into global and local components which mainly depend on the location of the measurement station and the local time. The global components include ionospheric potential, solar radiation, and natural radioactivity, and local components include atmospheric conductivity, space charge density, aerosols, and meteorological conditions. Numerous measurements of the intensity of surface EF have been conducted at marine, continental, polar and mountainous areas to explore global or local effects of atmospheric EF (Deshpande and Kamra, 2001; Harrison, 2013; Siingh *et al.*, 2013; Kamogawa *et al.*, 2015).

The atmospheric electric field is an important parameter used to characterize the global electrical circuit (Harrison, 2006; Aplin, 2012; Rycroft *et al.*, 2012). Generally, atmospheric EF shows a single intra-day oscillation over marine and polar areas where local effects are absent or low, in an effect referred to as the Carnegie curve (maximum around 19:00 UTC and minimum around 03:00 UTC) (Harrison, 2004; Harrison, 2013). Whipple (1929) presented a correlation between the Carnegie curve and the diurnal variation of the global thunderstorm area. The timing of the thunderstorm activity between the peaks in the values of electric field have a strong positive correlation, and the minimum in the Carnegie curve correlated with low

* Corresponding author.
Tel.: (86) 21-6564 3230; Fax: (86) 21-6564 2080
E-mail address: ttcheng@fudan.edu.cn

lightning activity over the Pacific at 4 UT (Williams and Sátori, 2004). Therefore the Carnegie curve mainly reflects the global effect, and it can be in marine and polar areas where local effects are absent or low. However, there are small differences in this pattern at a few sites, such as Maitri of Antarctica (Deshpande and Kamra, 2001). Aerosols can cause large variability of EF at continental sites by attaching or neutralizing small ions to reduce the air electric conductivity (Harrison, 2006; Silva *et al.*, 2014; Conceição *et al.*, 2016). Many studies have demonstrated the relationship between aerosols and atmospheric electricity. Adlerman and Williams (1996) reported a nonlinear relationship between aerosol and electrical conductivity over land. A positive correlation was found between the electric field and aerosol concentration (Jayaratne and Verma, 2004). Sheftel *et al.* (1994) showed that atmospheric EF and air conductivity are good indicators of anthropogenic atmospheric pollution. Kubicki *et al.* (2007) showed that the maximum annual variation of EF in winter resulted from high aerosol and dust concentrations at a land station.

Air pollutants such as nitrogen oxides (NO_x), sulfur dioxide (SO_2), ozone (O_3), carbon monoxide (CO) and particulate matter (PM) significantly, affect air quality (Chelani, 2013; Wang *et al.*, 2016). Recent studies revealed a high correlation between EF and air pollutants (Martín *et al.*, 2003; Silva *et al.*, 2016), and this effect was much stronger in winter. Air pollutants increase the ion recombination rate, causing a decrease of net ion concentration that reduces the air conductivity and increases the EF. Srivastava *et al.* (1972) observed that changes of EF and conductivity in the planetary boundary layer (PBL) are closely associated with dust, haze, and the local meteorological conditions. Piper and Bennett (2012) found that shallow convection and radiation fog can obviously influence the near-surface EF.

Atmospheric ions are mainly generated by the ionization of air molecules by ground and galactic cosmic radiation and radioactive materials such as Radon (Rn) and their short-lived progeny (Cheung *et al.*, 2015; Li *et al.*, 2015). Small ions are usually called molecular cluster ions, less than 1.6nm in size, and their recombination or attachment to aerosol particles allow to growth into intermediate (1.6–7.4 nm) and large (7.4–79 nm) ions (Pawar *et al.*, 2010; Li *et al.*, 2015). Additionally, the ion mobility decreases with increasing size (Tammet, 1995). Many studies have studied atmospheric ions and their contribution to particle formation (Harrison and Carslaw, 2003; Wilding and Harrison, 2005; Cheung *et al.*, 2015; Jayaratne *et al.*, 2016). Atmospheric ions also play a decisive role in atmospheric electrical variation. Pawar *et al.* (2005) measured air ions and found that large ions strengthen atmospheric electric conductivity. Harrison and Carslaw (2003) investigated the influence of atmospheric charged particles on aerosol and cloud microphysical processes, and examined the connection between atmospheric ionization rate and global cloudiness and weather systems.

Because they carry many electric charges, water droplets and rain-clouds can change EF drastically within a short time, especially during thunderstorms (Bennett and Harrison, 2007a). We screened out extreme weathers and only focused on fair weather to study near-surface atmospheric EF. We measured atmospheric EF and air ions in Shanghai from 2014 to 2015 to characterize their temporal variations and relevant influence factors. This information allows insights into the correlation of these parameters with pollution in urban environments with significant anthropogenic emissions of air ions.

OBSERVATION AND METHODOLOGY

Site Description

The observation site is located on the roof of a building about 20 m height above the ground on the campus of Fudan University (31.29°N, 121.51°E) in Shanghai of China, 40 km east of the East China Sea, surrounded by urban commercial and residential areas (Cheng *et al.*, 2015). The industrial emissions primarily come from a nearby steel plant and a power plant, and the nearest industrial sources are approximately 10 km away, primarily located in the northwest and the southeast (Li *et al.*, 2011).

Theory

In fair weather without intense atmospheric convection, according to Ohm's law, air electric conductivity (σ) is positively proportional to the current density (*J*), but inversely related to the atmospheric electric field (*E*).

$$J = \sigma E \tag{1}$$

Air electrical conductivity mainly depends on air ion concentration and mobility, especially for small ions, and the equation is as follows:

$$\sigma = e(n_+\mu_+ + n_-\mu_-) = 2en\mu \tag{2}$$

Specifically, n_+ and n_- refer to the concentrations of positive and negative ions, μ_+ and μ_- refer to positive and negative ion mobility, and e is the elementary charge. If bipolar ion concentrations are equal, the above equation can be simplified. Air ions are produced by galactic cosmic radiation and radioactive materials and are removed by recombination or attachment to aerosol particles. The stable state can be described as follows:

$$q - \alpha n^2 - n\beta Z = 0 \tag{3}$$

where q is the ion production rate, α is the ion-ion recombination coefficient, β is the ion-aerosol attachment coefficient, and Z is the aerosol number concentration. In case of severe pollution, aerosol particles at high concentration can result in increased ion-aerosol attachment to favor ion removal, i.e., $n\beta Z \gg \alpha n^2$, and then Eq. (3) can be simplified into Eq. (4).

$$n = q/\beta Z \tag{4}$$

Substituting Eq. (4) in the equation Eq. (2), and applying those results to Eq. (1), we obtain Eq. (5).

$$\mathrm{E} = J\beta Z/2q\mu e \tag{5}$$

In polluted air, the atmospheric electric field (EF) is positively proportional to the aerosol concentration (Z). Many measurements indicate similar results between electric field variations and aerosol concentrations (Retalis and Retalis, 1997; Harrison and Aplin, 2002; Silva *et al.*, 2014; Kubicki *et al.*, 2016).

Instrumentation and Observation

An electric-field mill (EFM-100, Boltek Corporation) utilizes the conductor in an electric field induced charge to measure the EF intensity at the surface of the earth. The electric-field mill was calibrated by the manufacturer with a parallel plate method before our use of the instrument for observation. The output signals were digitized and recorded every 0.5 seconds over the range of ± 20.0 × 10^3 V m^{-1}. It is very difficult to find an open place for observation, so the electric-field mill was installed on the roof of a barrier-free building. The EF on the building roof is stronger than on the ground due to the distortion effect caused by the surrounding cusp or steel structure building (Zhou *et al.*, 2010; Tan *et al.*, 2014).

The EF is often about several hundred V m^{-1} in fair weather, and becomes larger or negative in disturbed weathers such as thunderstorms, precipitation, and clouds (Bennett and Harrison, 2007a). In order to eliminate the effect of bad weathers, we collected data only for days with good weather (wind speed < 6 m s^{-1}, cloud coverage < 3/10 and no significant rainfall). This provided data for 54 days. No data was collected in February or November 2015 due to instrument maintenance.

An air ion mobility analyzer (DLY-71, Kilter Electronic Institute Co. Ltd., China) was used to measure air ion concentrations at the surface of the earth, with a magnitude resolution of 10 ions cm^{-3} and time resolution of 30 min. The instrument is able to measure small (< 1.6 nm), intermediate (1.6–7.4 nm) and large (7.4–79 nm) ions of both polarity (negative or positive), with mobilities of 3.2–0.4, 0.4–0.04 and 0.04–0.001 cm^2 V^{-1} s^{-1}, respectively.

Additionally, a set of micro pulse lidar (MPL, Sigma Space Corporation, USA) was applied to monitor the vertical profile of aerosol backscattering at 532 nm. The height of the planetary boundary layer (PBL) was obtained from MPL measurements using the classical Fernald algorithm and a lidar ratio of 30sr. The $PM_{2.5}$ concentration was measured using an on-line particle mass analyzer (Thermo SHARP-5030). A visibility monitor (VPF-730, Biral) was utilized to measure atmospheric visibility. Meteorological variables were measured at an automatic weather station (HydroMet™, Vaisala).

RESULTS AND DISCUSSION

Fair-Weather Atmospheric Electric Field

Fig. 1 shows the frequency distribution of hourly-averaged EF intensity in fair weather. The hourly EFs varied from 0 to 2 kV m^{-1}, with an average of 692 V m^{-1}. As show in the histograms, the hourly EFs were mainly concentrated in 500–800 V m^{-1}, similar to a Gaussian distribution with a fitting correlation coefficient of 0.98. The mean EFs were

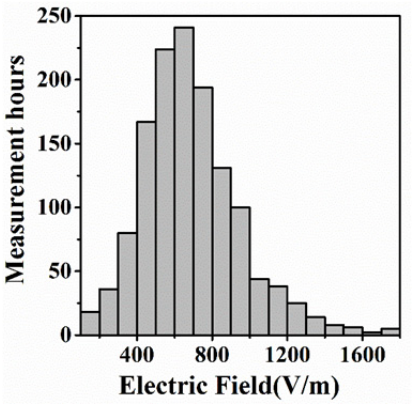

Fig. 1. Frequency distribution of hourly atmospheric electric field (EF) in fair weathers.

about 630, 660, 620 and 820 V m^{-1} in spring, summer, autumn and winter, respectively (Table 1). Higher EFs in winter and lower EFs in the summer were observed and are presented in Table 1 and Fig. 2. These results agree with those from other continental sites in the northern hemisphere (Retalis and Retalis, 1997; Israelsson and Tammet, 2001; Kastelis and Kourtidis, 2016). A possible explanation for this seasonal variability is likely increased aerosol concentration near the surface during winter, because the lack of strong surface heating and deep convective mixing means that pollution generated at the surface is confined to the near-surface where the EF is measured and not distributed upwards by summertime convective mixing (Bennett and Harrison, 2007b).

The hourly EFs show an obvious pattern of diurnal variation with multiple peaks (Fig. 2). Overall, the EFs were higher in the daytime than at night, especially in winter (> 1000 V m^{-1}). Generally, the EF peaks in winter appeared at 08:00–11:00 LT and 13:00–16:00 LT, and between these two peaks, the latter one was much higher. The EF peaks in the other three seasons occurred at 06:00–09:00 LT, 13:00–15:00 LT and 17:00–19:00 LT. The variation of the peaks in the daytime is possibly related to the effects of sunrise and sunset and human activities (Retalis and Retalis, 1997), particularly in spring, summer and autumn. At night, similar to the data from other continental stations, the higher EFs are likely due to the decrease of exchange layer heights (Latha, 2003). The bi- and multi-modal patterns were also observed at other continental sites (Harrison and Aplin, 2002; Kastelis and Kourtidis, 2016), and are largely affected by local factors of aerosols, meteorological conditions, space charge, and natural radioactivity. The atmospheric EFs also display a mono-modal pattern of diurnal variation at pristine places, such as in polar, oceanic, mountainous, and remote regions (Deshpande and Kamra, 2001; Israelsson and Tammet, 2001; Harrison, 2003; Panneerselvam *et al.*, 2007; Harrison, 2013; Siingh *et al.*, 2013; Xu *et al.*, 2013; Kamogawa *et al.*, 2015; Kastelis and Kourtidis, 2016).

The sunrise effect has been observed at tropical continental, rural and island areas (Latha, 2003). Law (1962) and Kamra (1982) reported that the EF increase is the response to the sunrise, positive space charge density increase and

Table 1. Annual and seasonal averages of electric field (EF), air ions and meteorological parameters.

	Winter	Spring	Summer	Autumn	Year
EF (V m^{-1})	825 ± 334	634 ± 184	668 ± 211	620 ± 223	692 ± 262
L^-	2408 ± 1166	2064 ± 920	1875 ± 772	2129 ± 1010	2119 ± 998
M^-	128 ± 43	87 ± 59	70 ± 33	80 ± 46	87 ± 50
S^-	148 ± 62	158 ± 49	112 ± 46	119 ± 56	130 ± 57
L^+	2267 ± 1205	1404 ± 916	2046 ± 1097	2155 ± 1050	2128 ± 1099
M^+	103 ± 41	101 ± 83	59 ± 40	65 ± 45	74 ± 50
S^+	132 ± 62	84 ± 84	115 ± 53	130 ± 53	126 ± 56
$PM_{2.5}$	84 ± 55	50 ± 27	45 ± 20	46 ± 26	57 ± 40
PM_{10}	123 ± 68	75 ± 34	66 ± 26	72 ± 38	85 ± 51
Visibility (km)	14 ± 9	24 ± 15	20 ± 10	23 ± 17	20 ± 13
T (°C)	6 ± 3	15 ± 7	29 ± 4	23 ± 4	18 ± 10
RH (%)	44 ± 15	53 ± 17	63 ± 15	57 ± 16	54 ± 17
Pressure (hPa)	1028 ± 4	1016 ± 8	1005 ± 2	1014 ± 5	1016 ± 10

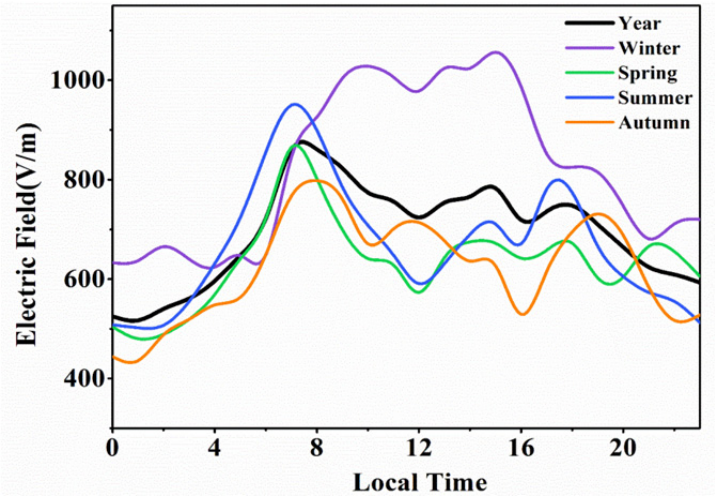

Fig. 2. Diurnal variation of mean atmospheric electric field (EF) in fair weathers on the seasonal and annual scales.

nocturnal inversion breakdown, but the conductivity rarely varies. Marshall *et al.* (1999) found that the sunrise effect is related with electrode layers and space charge transport. Additionally, morning solar heating leads to the dilution of the electrode layer built up during the night. More positive charges aggregate as a result of increasing vertical turbulent transportation and eventually give rise to EF increase (Marshall *et al.*, 1999). In our study, aerosol particles were positively correlated to EF, indicating that in addition to the sunrise effect, the influence of human activities on EF can be significant in the morning, especially in winter. In addition, the meteorological conditions are local influence factors on EF at the surface of the earth on smaller scales, particularly over polluted areas. The correlation and variance of EF and meteorological parameters are summarized in Table 2. Overall, the meteorological parameters showed a weak correlation with EF (Sig < 0.05), with wind direction the most correlated factor (0.54), and wind speed the least correlated factor (0.3). Generally, northwest, east, and west winds prevail in fair weathers, and the EFs mainly distribute in the west and east directions (Fig. 3).The EFs is lower in the east wind than the west wind, about 145 V m^{-1}. A possible reason for this is the east wind from oceanic areas carries clean air, but the west wind from inland areas carries more pollutants (Wang, 2013).

Air Ion Concentrations

Fig. 4 presents frequency histograms of the hourly positive and negative air ion concentrations, including large (L^+, L^-), intermediate (M^+, M^-), and small (S^+, S^-) ions. All ions present a similar Gaussian distribution, with fitting correlation coefficients of about 0.82–0.96. The L^+ and L^- ions are mostly in the range of 1500–2000 cm^{-3}, S^+ and S^- ions are in the range of 90–150 cm^{-3}, and M^+ ions are in the range of 20–60 cm^{-3} and M^- ions are in the range of 40–100 cm^{-3}. Table 1 summarizes the annual and seasonal averages of air ion concentrations in fair weather. Overall, the amount of large ions per volume is more than 20 times that of intermediate and small ions, and intermediate ions are the most rares. The mean concentrations of L^- and S^- are relatively higher in winter, autumn, and spring, and L^+ and S^+ are higher in winter, autumn and summer. The mean M^- concentrations are relatively higher in winter, and M^+ is higher in the winter and spring.

The correlation coefficients of the positive and negative ions were determined as 0.4, 0.71, and 0.35 for the large,

Table 2. Daily average of electric field (EF), meteorological parameters and their correlation coefficients (R) and ANOVA (Analysis of Variance).

Meteorological parameters	R	R Square	Adjusted R Square	ANOVA		Coefficients	
				F	Sig.	slope	intercept
Relative humidity (%)	0.464	0.215	0.200	13.995	0.000	–5.366	998.073
Temperature (°C)	0.397	0.158	0.141	9.546	0.003	–6.001	817.294
Pressure (hPa)	0.382	0.146	0.129	8.689	0.005	5.868	–5252.544
Wind Speed (m s^{-1})	0.298	0.089	0.068	4.298	0.044	85.557	545.380
Wind Direction (°)	0.536	0.287	0.273	20.573	0.000	1.119	521.813

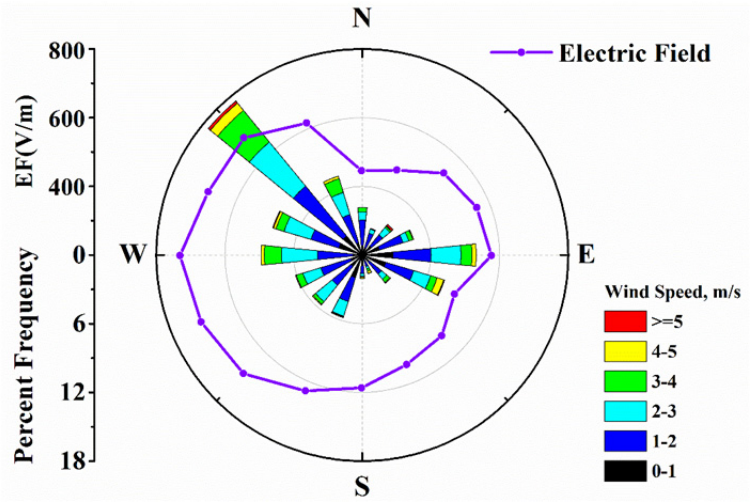

Fig. 3. Wind rose plot of atmospheric electric field (EF).

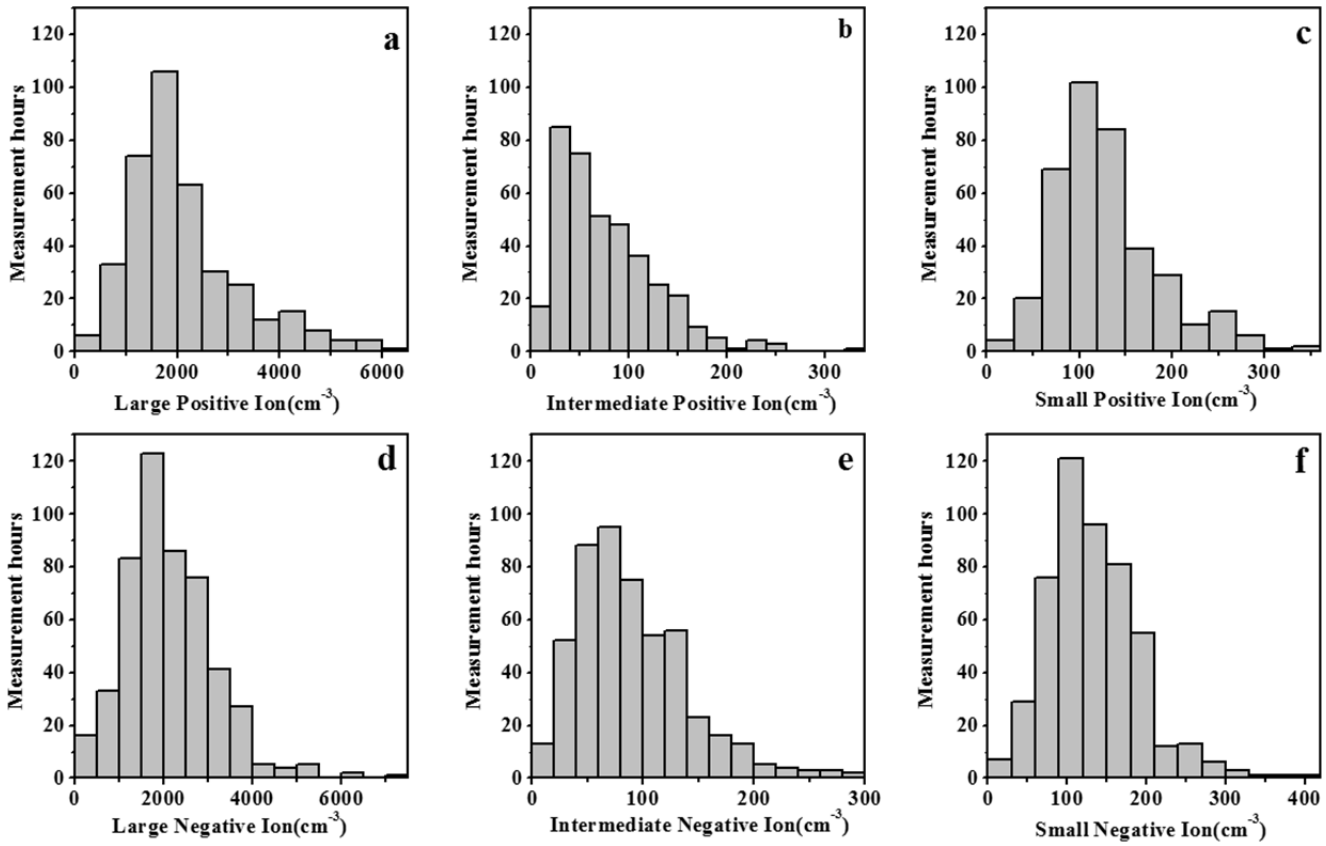

Fig. 4. Frequency distribution of hourly (a, b, c) positive and (d, e, f) negative ion concentrations in fair weathers.

intermediate and small ions, respectively (Fig. 5), indicating that are not derived from exactly the same sources, such as vehicle emissions in an urban environment (Cheung *et al.*, 2015). Each ion is assumed to be equally charged, and atmospheric large, intermediate, and small ions do not neutralize with each other. The electric polarity of large and small ions is usually negative in winter and spring (L^-/L^+ or S^-/S^+ = 1.0–1.9), and positive in summer and autumn (L^-/L^+ or S^-/S^+ = 0.9–1.0). The intermediate ions show negative polarity in winter, summer, and autumn (M^-/M^+ = 1.1–1.3) but positive polarity in summer (M^-/M^+ = 0.86). Overall, in terms of measured ions, the atmosphere shows weak negative polarity in winter and spring, and weak positive polarity in summer and autumn.

Fig. 6 depicts the diurnal variations of hourly air ion concentrations. Overall, air ion concentrations are relatively higher in the daytime compared to those at night, possibly due to the ionization effect by solar radiation. The L^+ and S^+ begin to rise at 6:00 LT, and subsequently reach the first peak at around 9:00 LT, the second peak at around 13:00 LT, and the third peak around 20:00 LT before reaching a minimum at midnight. Similarly, L^- and S^- peaks occur around 10:00, 16:00, and 19:00 LT, but the L^- and S^- peaks are lower and last longer than those for L^+ and S^+. For the intermediate ions, the M^- concentration is almost larger than the M^+ concentration, and their peaks appear during 5:00–8:00, 10:00–15:00 and 19:00–20:00 LT. In terms of polarity, the large and small ions show positive polarity at around 0:00–4:30, 8:00–9:00 and 12:00–14:30 LT, but negative polarity dominates during the other times. However, the intermediate ions show mostly negative polarity throughout day.

The meteorological conditions influence the positive and negative ions (Fig. 7). As temperature, visibility, and wind speed increase, the large, intermediate and small ions become denser per volume, but the opposite trend is observed when the relative moisture rises. Moreover, the intermediate ions exhibit a greater sensitivity (i.e., slope) to varying meteorological parameters than the small and large ions. Temperature increases will strengthen the ionization process to increase the concentration of ions. However, a high relative humidity, a high concentration of amount of water molecules per unit volume, may cause a high collision probability and an increased combination rate between water molecules (Retalis *et al.*, 2009; Hirsikko *et al.*, 2011; Li, 2015). Therefore, the concentration of air ions is higher under conditions of low relative humidity or high temperature.

Fig. 8 presents the wind rose plots of positive and negative air ions. In brief, since the wind direction and wind speed can affect the transportation of pollutants, especially particles,

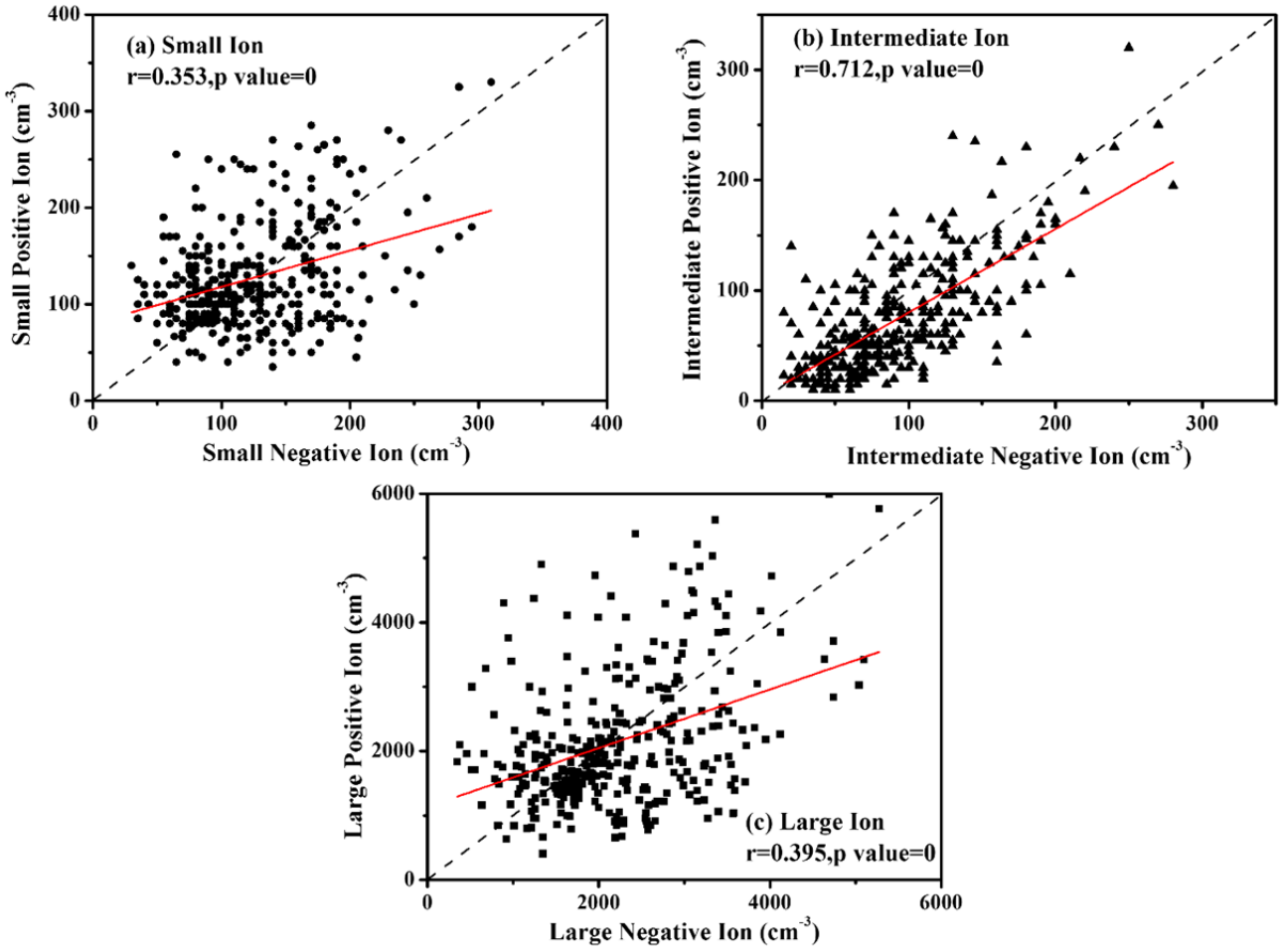

Fig. 5. Scatter plots of negative and positive (a) large, (b) intermediate and (c) small ions.

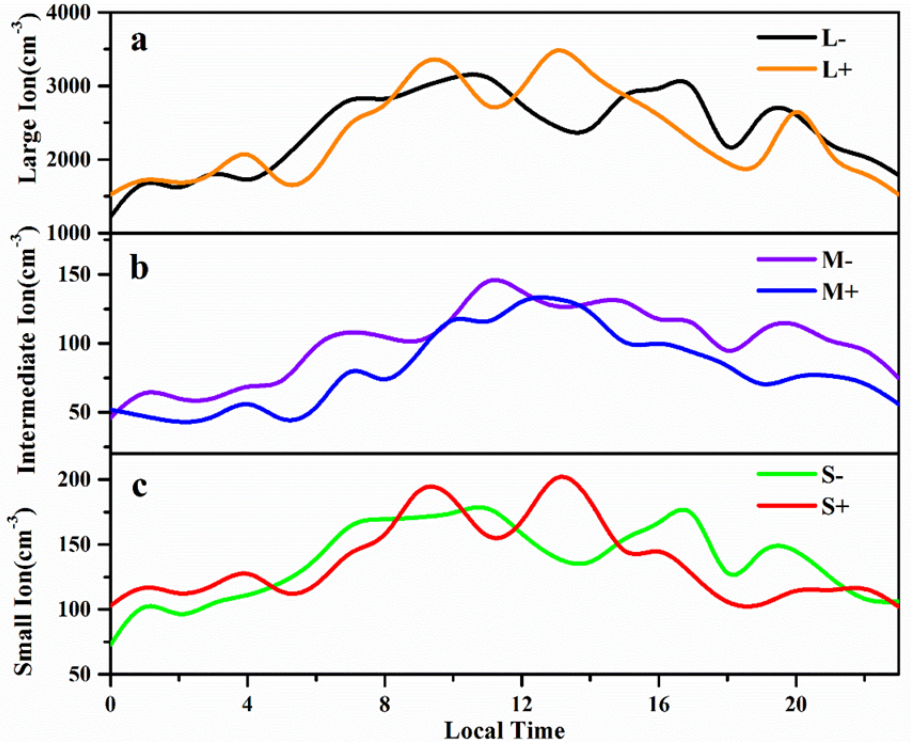

Fig. 6. Diurnal variations of mean negative and positive (a) small, (b) intermediate and (c) large air ions.

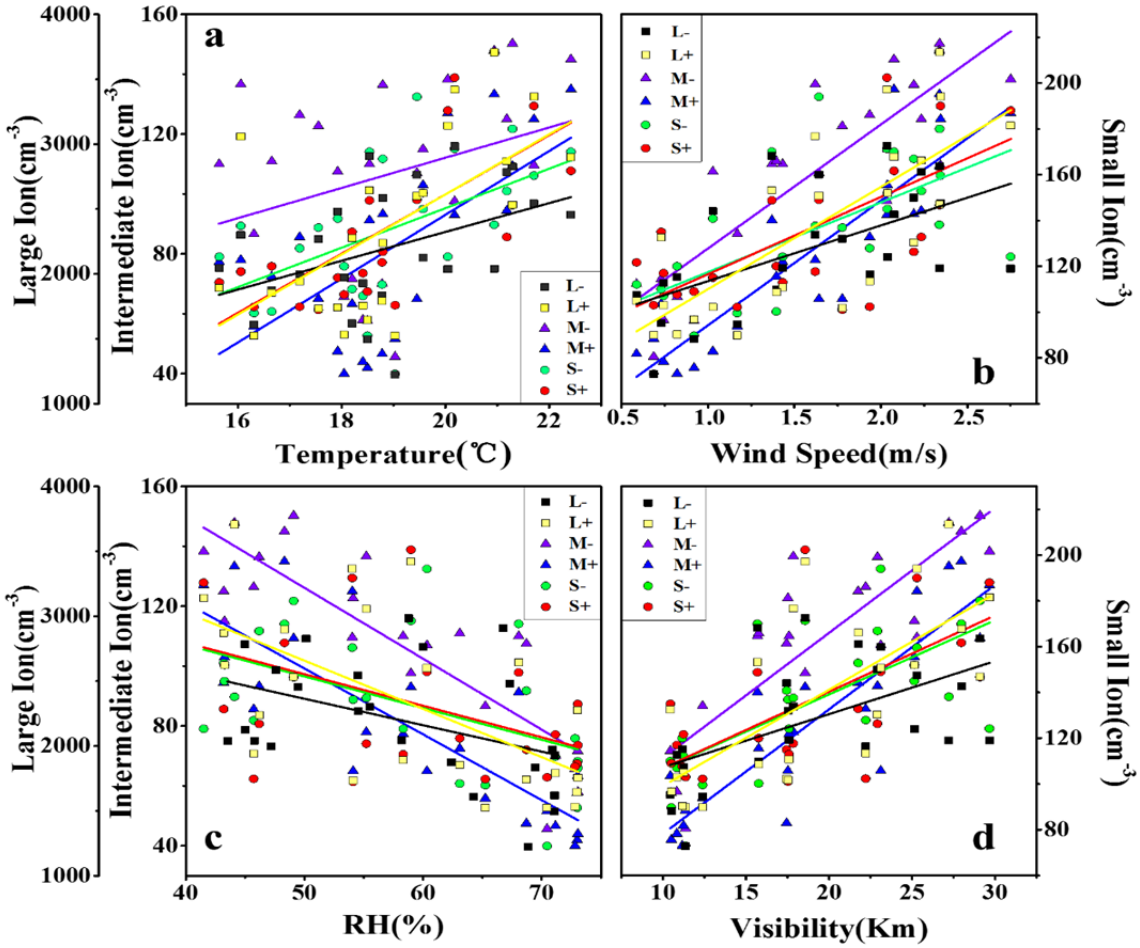

Fig. 7. Scatter plots of hourly large, intermediate and small ions vs. meteorological parameters.

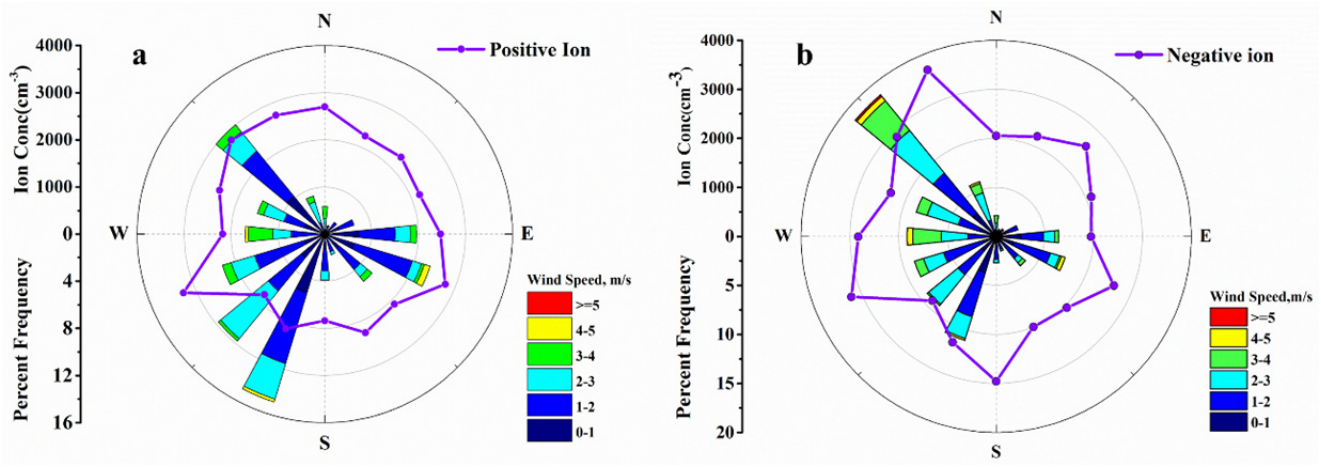

Fig. 8. Wind rose plots of (a) positive and (b) negative air ions.

the air ion density changes accordingly. Positive ions prevail in the southwest (WWS), northwest (WN), north (N), and southeast (EES), and negative ions are prominent in the southwest (WWS), northwest (NWN), northeast (EN), southeast (EES) and south (S). In contrast, positive ions have a relatively weaker dependency on wind directions than negative ions, consistent with previous results (Cheung *et al.*, 2015).

In these result, there was a greater influence of the wind on air ions compared to the effect on atmospheric EF, but this finding may reflect the lower amount of available air ion data as a result of low time resolution (30 min).

Atmospheric Electric Field and Air Ions in Pollution

Aerosol particles can attach to or neutralize small ions to decrease ions density and conductivity, thus increasing the atmospheric electric field (Law, 1962; Kamra, 1982). Air ions involved in particle formation and growth by recombination or attachment in an urban environment (Cheung *et al.*, 2015). In fact, the atmospheric electric field is linked closely with pollutants, especially particles and their precursors, and can be viewed as an indicator of atmospheric pollution (Sheftel *et al.*, 1994; Guo *et al.*, 1996). Here, we analyzed the variation of the electric field, air ions, and pollutants in pollution.

Fig. 9 shows a time series of atmospheric EF, air ion concentrations, and meteorological parameters from 11 to 13 October 2015. During this period, the PBL height was close to 500 m, the relative humidity was close to 60%, atmospheric visibility gradually decreased, and $PM_{2.5}$ increased from 23 to 139 μg m^{-3}, indicating that the air pollution worsened over this time period. In addition, despite fluctuation, the EF showed a slow growth trend (Fig. 9(c)). There were no obvious change in the distribution of the large, intermediate, and small air ions (Figs. 9(d)–9(f)).

On the 11th of October, the $PM_{2.5}$ was measured at 54 μg m^{-3}, the PBL height was about 567 m, and the EF waves were about 542 V m^{-1}. In the morning, due to the sunrise effect and strengthened air vertical turbulent and transportation, the PBL height increased from 300 m to 800 m. More ions, especially positive ions were generated with increased amounts of aerosols. At our measurement site, human activities such as motor vehicle emissions and electrical appliances like transformers and air conditioners are the major sources of atmospheric ions and charged particles (Jayaratne *et al.*, 2016). Under natural, stable conditions, atmospheric ions are present at concentrations of about 300–400 cm^{-3} but the concentration may increase to a few thousand cm^{-3} in the presence of anthropogenic ion sources such as motor vehicle exhaust (Maricq, 2006; Ling *et al.*, 2010) and overhead power lines (Fews *et al.*, 1999; Jayaratne *et al.*, 2008). In this study, a higher concentration of positive and negative ions was found as shown in Fig. 9. The higher amount of positive ions relative to negative may be explained in terms of the higher mobility of negative ions. Negative ions have a higher efficiency of ion neutralization and, therefore, their lifetime and concentration are generally lower than those of positive ions (Kolarž *et al.*, 2009). The lifetimes of small ions are significantly reduced in more polluted environments because ions with higher mobility (negative) will be neutralized faster due to their ability to attach to particles (Jayaratne *et al.*, 2016). Therefore, the concentration of positive ions is higher than negative ions as a result of growing aerosols from human activities. The first peak of EF appeared at 7:00 LT, and the second peak was between 15:00 to 20:00 LT. This may be because more particles consume small ions, and then reduce the air conductivity and enhance EF. From 12 to 14, October, the EF was far higher than that of fair weather conditions and ranged from 154 V m^{-1} to 1458 V m^{-1} with a larger fluctuation. The $PM_{2.5}$ and atmospheric visibility showed linear correlation with EF, with coefficients of 0.5 and –0.4, respectively. In summary, our results indicate that particles under polluted conditions are greatly influential towards the atmospheric electric field.

CONCLUSIONS

One-year measurement of the atmospheric electric field (EF), air ions and pollutants was employed to explore temporal variations and interactions of these parameters. The atmospheric EF was observed to be generally higher in

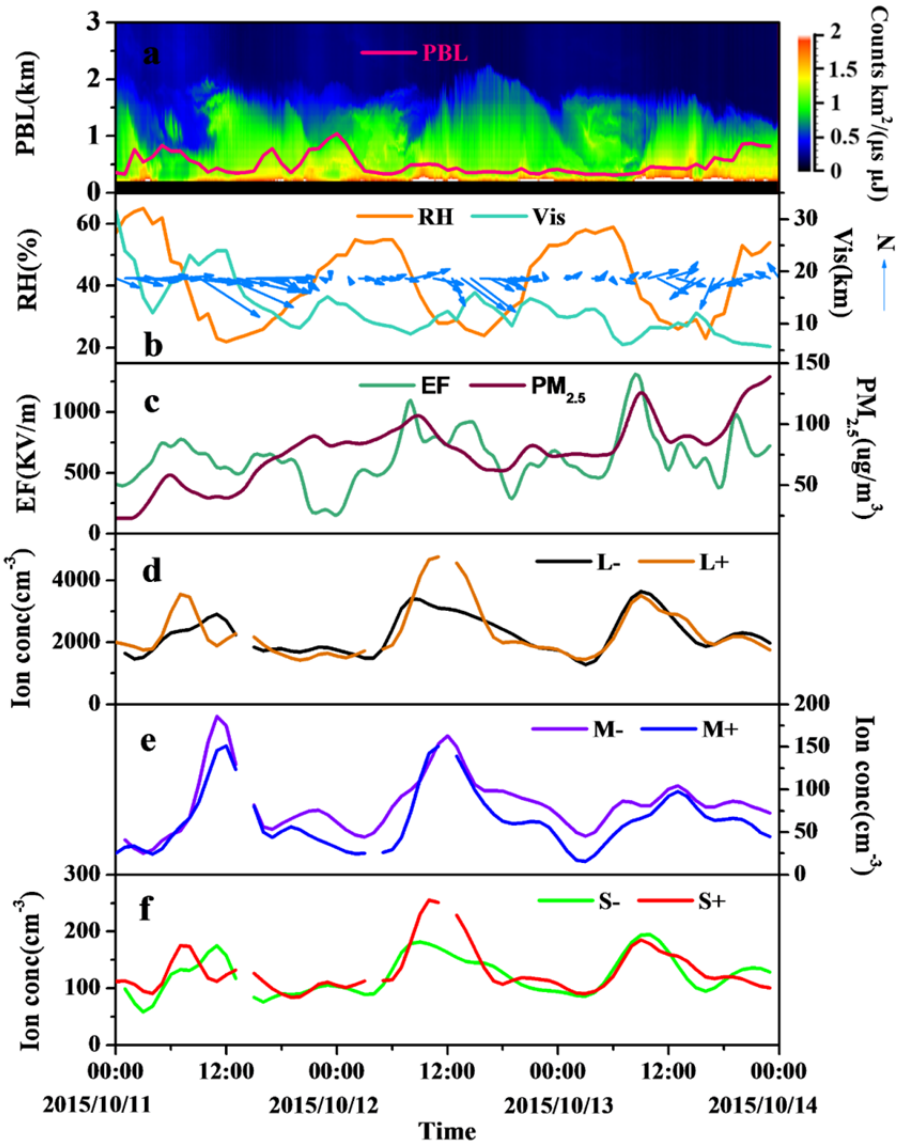

Fig. 9. Time series of atmospheric electric field (EF), air ion concentrations and meteorological parameters from 11 to 13 October 2015.

winter than in the other three seasons. The EF in fair weather exhibited a multimodal oscillation during the day due to the sunrise effect and air vertical convection. This is consistent with the observation results at other continental stations in the northern hemisphere.

In addition to be the meteorological parameters, aerosol particles play a significant role in atmospheric EF variation by affecting air ions and air conductivity, especially in winter. In contrast, the EF fluctuates more in polluted conditions and less in cloudless and clean conditions. In polluted periods, the atmospheric EF increased gradually with increasing amounts of $PM_{2.5}$, and roughly reflects the trend of pollution.

ACKNOWLEDGMENTS

This research is supported by the National Natural Science Foundation of China (41475109, 21577021, 21377028, 91637101), the National Key Research and Development Program of Ministry of Science and Technology (2016YFC0202003), and partly by the Science and Technology Commission of Shanghai Municipality (16ZR1431700) and the Jiangsu Collaborative Innovation Center for Climate Change.

REFERENCES

Adlerman, E.J. and Williams, E.R. (1996). Seasonal variation of the global electrical circuit. *J. Geophys. Res.* 101: 29679–29688.

Aplin, K.L. (2012). Smoke emissions from industrial western Scotland in 1859 inferred from Lord Kelvin's atmospheric electricity measurements. *Atmos. Environ.* 50: 373–376.

Bennett, A.J. and Harrison, R.G. (2007a). Atmospheric electricity in different weather conditions. *Weather* 62: 277–283.

Bennett, A.J. and Harrison, R.G. (2007b). Variability in surface atmospheric electric field measurements. *J. Phys. Conf. Ser.* 142: 012046.

Campbell, J.R., Hlavka, D.L., Welton, E.J., Flynn, C.J., Turner, D.D., Spinhirne, J.D., Scott, V.S. and Hwang, I.H. (2002). Full-time, eye-safe cloud and aerosol lidar observation at atmospheric radiation measurement program sites: Instruments and data processing. *J. Atmos. Oceanic Technol*. 19: 431–442.

Chelani, A.B. (2013). Study of extreme CO, NO_2 and O_3 concentrations at a traffic site in Delhi: Statistical persistence analysis and source identification. *Aerosol Air Qual. Res.* 13: 377–384.

Cheng, T., Xu, C., Duan, J., Wang, Y., Leng, C., Tao, J., Che, H., He, Q., Wu, Y., Zhang, R., Li, X., Chen, J., Kong, L. and Yu, X. (2015). Seasonal variation and difference of aerosol optical properties in columnar and surface atmospheres over Shanghai. *Atmos. Environ*. 123: 315–326.

Cheung, H.C., Chou, C.C.K., Jayaratne, E.R. and Morawska, L. (2015). Impact of particle formation on atmospheric ions and particle number concentrations in an urban environment. *Atmos. Res*. 157: 127–136.

Conceição, R., Melgão, M., Silva, H.G., Nicoll, K., Harrison, R.G. and Reis, A.H. (2016). Transport of the smoke plume from Chiado's fire in Lisbon (Portugal) sensed by atmospheric electric field measurements. *Air Qual. Atmos. Health* 9: 275–283.

Deshpande, C.G. and Kamra, A.K. (2001). Diurnal variations of the atmospheric electric field and conductivity at Maitri, Antarctica. *J. Geophys. Res*. 106: 14207–14218.

Fews, A.P., Henshaw, D.L., Wilding, R.J. and Keitch, P.A. (1999). Corona ions from power lines and increased exposure to pollutant aerosols. *Int. J. Radiat. Biol.* 75: 1523–1531.

Guo, Y., Barthakur, N.N. and Bhartendu, S. (1996). Using atmospheric electrical conductivity as an urban air pollution indicator. *J. Geophys. Res*. 101: 9197–9203.

Harrison, R.G. (2004). Long-term measurements of the global atmospheric electric circuit at Eskdalemuir, Scotland, 1911-1981. *Atmos. Res*. 70: 1–19.

Harrison, R.G. (2006). Urban smoke concentrations at Kew, London, 1898–2004. *Atmos. Environ*. 40: 3327–3332.

Harrison, R.G. and Aplin, K.L. (2002). Mid-nineteenth century smoke concentrations near London. *Atmos. Environ*. 36: 4037–4043.

Harrison, R.G. (2013). The carnegie curve. *Surv. Geophys*. 34: 209–232.

Harrison, R.G. and Carslaw, K.S. (2003). Ion-aerosol-cloud processes in the lower atmosphere. *Rev. Geophys*. 41: 181–207.

Hirsikko, A., Nieminen, T., Gagné, S., Lehtipalo, K., Manninen, H.E., Ehn, M., Hõrrak, U., Kerminen, V.M., Laakso, L., McMurry, P.H., Mirme, A., Mirme, S., Petäjä, T., Tammet, H., Vakkari, V., Vana, M. and Kulmala, M. (2011). Atmospheric ions and nucleation: A review of observations. *Atmos. Chem. Phys.* 11: 767–798.

Israelsson, S. and Tammet, H. (2001). Variation of fair weather atmospheric electricity at Marsta Observatory, Sweden, 1993-1998. *J. Atmos. Terr. Phys.* 63: 1693–1703.

Jayaratne, E.R. and Verma, T.S. (2004). Environmental aerosols and their effect on the Earth's local fair-weather electric field. *Meteorol. Atmos. Phys*. 86: 275–280.

Jayaratne, E.R., Fatokun, J.F. and Morawska, L. (2008). Air ion concentrations under overhead high-voltage transmission lines. *Atmos. Environ.* 42: 1846–1856.

Jayaratne, E.R., Ling, X. and Morawska, L. (2016). Charging state of aerosols during particle formation events in an urban environment and its implications for ion-induced nucleation. *Aerosol Air Qual. Res.* 16: 348–360.

Kamogawa, M., Suzuki, Y., Sakai, R., Fujiwara, H., Torii, T., Kakinami, Y., Watanabe, Y., Sato, R., Hashimoto, S., Okochi, H., Miura, K., Yasuda, H., Orihara, Y. and Suzuki, T. (2015). Diurnal variation of atmospheric electric field at the summit of Mount Fuji, Japan, distinctly different from the Carnegie curve in the summertime. *Geophys. Res. Lett.* 42: 3019–3023.

Kamra, A.K. (1982). Fair weather space charge distribution in the lowest 2m of the atmosphere. *J. Geophys. Res*. 87: 4257–4263.

Kastelis, N. and Kourtidis, K. (2016). Characteristics of the atmospheric electric field and correlation with CO_2 at a rural site in southern Balkans. *Earth Planets Space* 68: 1–15.

Kolarž, P., Filipović, D. and Marinković, B. (2009). Daily variations of indoor air-ion and radon concentrations. *Appl. Radiat. Isot.* 67: 2062–2067.

Kubicki, M., Michnowski, S. and Myslek-Laurikainen, B. (2007). Seasonal and daily variations of atmospheric electricity parameters registered at the Geophysical Observatory at Swider (Poland) during 1965-2000. Proceedings of the 13th International Conference on Atmospheric Electricity. pp. 50–53.

Kubicki, M., Odzimek, A. and Neska, M. (2016). Relationship of ground-level aerosol concentration and atmospheric electric field at three observation sites in the Arctic, Antarctic and Europe. *Atmos. Res*. 178–179: 329–346.

Latha, R. (2003). Diurnal variation of surface electric field at a tropical station in different seasons a study of plausible influences. *Earth Planets Space* 55: 677–685.

Law, J. (1962). The ionisation of the atmosphere near the ground in fair weather. *Q. J. R. Meteorolog. Soc.* 89: 107–121.

Li, P., Li, X., Yang, C., Wang, X., Chen J. and Collett Jr., J.L. (2011). Fog water chemistry in Shanghai. *Atmos. Environ*. 45: 4034–4041.

Li, Y., Guo, X., Wang, T., Zhao, Y., Zhang, H. and Wang, W. (2015). Characteristics of atmospheric small ions and their application to assessment of air quality in a typical semi-arid city of northwest China. *Aerosol Air Qual. Res.* 15: 865–874.

Ling, X., Jayaratne, R. and Morawska, L. (2010). Air ion concentrations in various urban outdoor environments. *Atmos. Environ*. 44: 2186–2193.

Maricq, M. (2006). On the electrical charge of motor vehicle exhaust particles. *J. Aerosol Sci.* 37: 858–874.

Marshall, T.C., Rust, W.D., Stolzenburg, M., Roeder, W.P.

and Krehbiel, P.R. (1999). A study of enhanced fair-weather electric fields occurring soon after sunrise. *J. Geophys. Res*. 104: 24455–24469.

Martín, L.D., Diez, E.G., Dávila, F.D.P. and Soriano, L.R. (2003). Relationship between the atmospheric electric field (AEF) and air pollution in the lower levels of the atmosphere. Proceedings of 12th ICAE, p. 365.

Panneerselvam, C., Selvaraj, C., Jeeva, K., Nair, K.U., Anilkumar, C.P. and Gurubaran, S. (2007). Fairweather atmospheric electricity at Antarctica during local summer as observed from Indian station, Maitri. *J. Earth Syst. Sci.* 116: 179–186.

Pawar, S.D., Siingh, D., Gopalakrishnan, V. and Kamra, A.K. (2005). Effect of the onset of southwest monsoon on the atmospheric electric conductivity over the Arabian Sea. *J. Geophys. Res*. 110: 257–266.

Pawar, S.D., Meena, G.S. and Jadhav, D.B. (2010). Diurnal and seasonal air ion variability at rural station Ramanandnagar (17°2′N, 74°E), India. *Aerosol Air Qual. Res.* 10: 154–166.

Piper, I.M. and Bennett, A.J. (2012). Observations of the atmospheric electric field during two case studies of boundary layer processes. *Environ. Res. Lett*. 7: 14017–14020.

Retalis, A., Nastos, P. and Retalis, D. (2009). Study of small ions concentration in the air above Athens, Greece. *Atmos. Res.* 91: 219–228.

Retalis, D. and Retalis, A. (1997). The atmospheric electric field in Athens-Greece. *Meteorol. Atmos. Phys*. 63: 235–241.

Sheftel, V.M., Chernyshev, A.K. and Chernysheva, S.P. (1994). Air conductivity and atmospheric electric field as an indicator of anthropogenic atmospheric pollution. *J. Geophys. Res*. 99: 10793–10795.

Siingh, D., Singh, R.P., Gopalakrishnan, V., Selvaraj, C. and Panneerselvam, C. (2013). Fair-weather atmospheric electricity study at Maitri (Antarctica). *Earth Planets Space*. 65: 1541–1553.

Silva, H.G., Conceição, R., Melgão, M., Nicoll, K., Mendes, P.B., Tlemçani, M., Reis, A.H. and Harrison, R.G. (2014). Atmospheric electric field measurements in urban environment and the pollutant aerosol weekly dependence. *Environ. Res. Lett*. 9: 114025.

Silva, H.G., Conceição, R., Khan, M.A.H., Matthews, J.C., Wright, M.D., Collares-Pereira, M. and Shallcross, D.E. (2016). Atmospheric electricity as a proxy for air quality: Relationship between potential gradient and pollutant gases in an urban environment. *J. Electrostat.* 84: 32–41.

Srivastava, G.P., Huddar, B.B. and Mani, A. (1972). Electrical conductivity and potential gradient measurements in the free atmosphere over India. *Pure Appl. Geophys*. 100: 81–93.

Tammet, H. (1995). Size and mobility of nanometer particles, clusters and ions. *J. Aerosol Sci*. 26: 459–475.

Tan, Y., Zhang, D., Guo, X., Zhou, B. and Yang, Y. (2014). Numerical simulation of effects of shape of axial symmetry buildings on electric field distortion. *Chin. J. Radio Sci*. 29: 1219–1224 (in Chinese).

Wang, H., Zhu, B., Shen, L., Xu, H., An, J., Pan, C., Li, Y. and Liu, D. (2016). Regional characteristics of air pollutants during heavy haze events in the Yangtze River Delta, China. *Aerosol Air Qual. Res*. 16: 2159–2171.

Wang, Q. (2013). Study of air pollution transportation source in Shanghai using trajectory model. *Res. Environ. Sci*. 26: 357–363 (in Chinese).

Whipple, F.J.W. (1929). On the association of the diurnal variation of the electric potential gradient in fine weather with the distribution of thunderstorms over the globe. *Q. J. R. Meteorolog. Soc.* 55: 351–361.

Wilding, R.J. and Harrison, R.G. (2005). Aerosol modulation of small ion growth in coastal air. *Atmos. Environ*. 39: 5876–5883.

Williams, E.R. and Sátori, G. (2004). Lightning, thermodynamic and hydrological comparison of the two tropical continental chimneys. *J. Atmos. Terr. Phys.* 66: 1213–1231.

Xu, B., Huang, C. and Chen, B. (2013). Observation of the variations of the atmospheric electric field at YBJ, Tibet. *Meteorol. Atmos. Phys*. 121: 99–107

Zhang, R., Li, X., Chen, J., Kong, L. and Yu, X. (2015). Seasonal variation and difference of aerosol optical properties in columnar and surface atmospheres over Shanghai. *Atmos. Environ*. 123: 315–326.

Zhou, B., Jiang, H., Yang, B., Guo, J. and Zhu, K.E. (2010). Influence of surface features on atmospheric electric field near ground. *Chin. J. Radio Sci*. 25: 839–844 (in Chinese).

Received for review, July 30, 2017
Revised, October 26, 2017
Accepted, November 13, 2017